J Appl Electrochem (2014) 44:621–629
DOI 10.1007/s10800-014-0666-2

RESEARCH ARTICLE

# Electrochemically mediated atom transfer radical polymerization of iminodiacetic acid-functionalized poly(glycidyl methacrylate)grafted at carbon fibers for nano-nickel recovery from spent electroless nickel plating baths

**Guan-Ping Jin · Ya Fu · Xing-Chen Bao · Xiao-Shuang Feng · Yan Wang · Wen-Hong Liu**

Received: 28 October 2013 / Accepted: 10 January 2014 / Published online: 28 January 2014


**Abstract** In this work, iminodiacetic acid-functionalized poly(glycidyl methacrylate)grafted carbon fibers (CCFs) were prepared by electrochemically mediated atom transfer radical polymerization (eATRP) for nano-nickel recovery from spent electroless nickel (EN) plating baths. The adsorption behaviors of $Ni^{2+}$ were investigated at CCFs in the spent EN plating baths. The adsorption kinetics perfectly fitted pseudo-second order model with a chemisorption process. The thermodynamic parameters suggested that adsorption was feasible, spontaneous, and endothermic. The adsorption maximum capacity was 0.908 mM $g^{-1}$ under optimum conditions (pH 5.2, 50 °C and 40 min). The present materials were carefully characterized by the Fourier transform infrared spectroscopy, X-ray diffraction, field emission scanning electron microscope, and electrochemical techniques. Experimental results showed that CCFs were successfully prepared, which were efficient adsorbent and support for nano-nickel recovery from the spent EN plating baths.

G.-P. Jin (✉) · Y. Fu · X.-C. Bao · Y. Wang · W.-H. Liu
Department of Application Chemistry of School of Chemical Engineering, Hefei University of Technology, Hefei 230009, People's Republic of China
e-mail: jgp@hfut.edu.cn

X.-S. Feng
College of Chemistry & Chemical Engineering, Anhui University, Hefei 230601, People's Republic of China

X.-S. Feng
Eco-Efficient Product & Process Laboratory (E2P2L), UMI 3464, Research & Innovation Center in Shanghai (RICS), Solvay (China) Co., Ltd, 3966 Jindu Road, Shanghai 201108, People's Republic of China

**Keywords:** Electrochemically mediated atom transfer radical polymerization · Chelating carbon fibers · Recovery · Spent EN plating baths

## 1 Introduction

Environmental contaminations for heavy metals are caused by several industries such as metal plating, mining, painting, and car radiator manufacturing [1, 2]. These heavy metals may cause cancers and other serious diseases [3]. Adsorption is one of the methods commonly used to remove heavy metal ions from various aqueous solutions due to conveniency and economy. Various adsorbents including activated carbon fibers (CFs), oxide minerals, chelated resins, cellulose, and protein have been used to remove the heavy metal ions [4–8]. Among these, CFs are obviously convenient for separation operation; moreover, CFs have outstanding mechanical properties, chemical stability, and conduction. These allow possibility of various functional modifications by electrochemical method, organic synthesis, r-rays irradiation aid, and wet spinning technique [9–12]. Since original CFs display poor uptake and selectivity on the heavy metal ions removal, the preparation of chelating CFs have attracted much attention. For example: Cyclam-functionalized polyglycidyl methacrylate/CFs formed by atom transfer radical polymerization for $Cu^{2+}$ uptake [9]; tetraoxalyl ethylenediamine melamine chelated resin/CFs formed by radical polymerization for $Ni^{2+}$ recovery [2]; ethylenediamine/4-(2-pyridylazo)-1,3-benzenediol/CFs formed by Mannich reaction for $Hg^{2+}$, $Pb^{2+}$, $Cd^{2+,}$ $Zn^{2+}$, $Ni^{2+}$, and $Cu^{2+}$ adsorption [10]; amine/CFs formed by r-rays irradiation aid for $Hg^{2+}$ removal [11]; and carboxymethylated polyallylamine/CFs, carboxymethylated polyethyleneimine/

CFs, diallylamine hydrochloride/maleic acid/CFs formed by wet spinning technique for $Cd^{2+}$, $Co^{2+}$, $Cr^{3+}$, $Cu^{2+}$, $Fe^{3+}$, $Mn^{2+}$, $Ni^{2+}$, $Pb^{2+}$, $Ti^{4+}$, and $Zn^{2+}$ removal [12]. Although many studies have successively prepared various chelating CFs, the development on chelating CFs always are significant for the effective recovery of heavy metal ions.

On the other hand, as a new and efficient way to conduct controlled/"living" radical polymerization, atom transfer radical polymerization (ATRP) was independently discovered by Sawamoto and Wang [13, 14]. According to the synthesis method, ATRP could be divided into organic and electrochemical synthesis. $Cu^{+}/Cu^{2+}$ complex is used as catalyst with high monomer concentrations in standard ATRP (organic synthesis), and the efficient use of monomers is lower. Meanwhile the ATRP is usually carried out in an inert atmosphere because oxygen will oxidize $Cu^{+}$ to the deactivating $Cu^{2+}$ species [15, 16]. In recent years, the ATRP process has been expanded via activators generated by electron transfer (eATRP). Under a certain potential, the $Cu^{2+}$ could be reduced to $Cu^{+}$. ATRP process could be conducted by a very active copper catalyst in several ppm concentrations [9, 12, 15]. In comparison with the organic synthesis, tolerance to limited $O_2$ is the advantage of electrochemical synthesis, as we know that methyl methyl methacrylate, tert-butyl acrylate, acrylate esters, and isobutyl methacrylate could be controllably polymerized at CFs by standard ATRP [17–19]. Well-controlled or living polymerization of glycidyl methacrylate has not been reported at CFs by eATRP up to now. Moreover, poly(glycidyl methacrylate)-iminodiacetic acid chelate resin has been concerned by some researchers because of strong chelation with metal ions, which has been applied to the removal of $Cu^{2+}$, $Cr^{3+}$, $Zn^{2+}$, and $Co^{2+}$ [20–22], and the support of catalyst [23, 24]. In present work, iminodiacetic acid immobilized poly(glycidyl methacrylate) grafted on carbon fibers (CCFs) was prepared first using eATRP method, the uptake of $Ni^{2+}$ was investigated at CCFs in an actual spent EN plating baths, and the nano-nickel coated CFs (Ni/CFs) could be obtained by electrodeposition in situ.

## 2 Experimental

### 2.1 Chemicals and apparatus

Polyacrylonitrile-carbon fibers (CFs) were obtained from Dingfeng Carbon Fibers Fabrication Company of Yixing (China, Wuxi), one truss CFs have about 3,000 branches with a diameter of 7 ± 1 μm, it was been snipped at 8 mm long in following experiments. 1-(4-Aminophenyl) ethanol, glycidyl methacrylete (GMA), iminodiacetic acid, *N*,*N*-dimethylformamide, 2,2′-bipyridine (Bpy), sodium fluoroborate ($NaBF_4$), fluoroboric acid ($HBF_4$), tetrabutyl ammonium fluoride boric acid ($NBu_4BF_4$), tetramethyl ammonium bromide, acetonitrile, 1-(4-aminophenyl) ethanol, and all other chemicals were Chemical Reagent Company of Shanghai products (China, Shanghai). A stock solution of 1.5 mM EDTA was prepared and standardized against a solution of $MgSO_4{\cdot}7H_2O$ using Eriochrome Black-T (EBT) as an indicator. $HNO_3$ and NaOH were used to change the acidity of the medium. The composition of spent EN plating baths was shown in Table 1 (S1), the content for [$Ni^{2+}$] is 0.171 M, and the pH is 4.8.

All electrochemical experiments were performed with a CH660B electrochemical workstation (Chenhua, Shanghai, China). A conventional three-electrode electrochemical system was used for all electrochemical experiments, which consisted of a working electrode (CFs), a twisted platinum wire counter electrode, and a saturated calomel reference electrode (SCE). Field emission scanning electron microscope (FE–SEM) images were obtained on a JSM-600 field emission scanning electron microanalyser (JEOL, Japan). X-ray diffraction (XRD) data of the samples were collected using a Rigaku D/MAX-rB diffractometer with Cu Kα radiation. Infrared spectra were measured at IR 200 (America Nicolet). The pH meter model was measured at HI 255 (Shanghai Leici Instruments). The average pore sizes and the specific surface area of CCFs were measured using Nova 2200e Surface Area & Pore Size Analyzer (Quantachrome Instrument, America).

### 2.2 Preparation of CCFs

The preparation of iminodiacetic acid-functionalized poly(glycidyl methacrylate)grafted carbon fibers (CCFs) could be clarified as follow: First, synthesis of the diazonium salt bearing eATRP initiating group. The diazonium salt $BF_4^-$, $^{+}N_2$–$C_6H_4$–$CH(CH_3)$–Br (D1) was prepared in line with Ref [25]. It was obtained in one pot from 1 g 1-(4-aminophenyl) ethanol to 5 mL 48 % HBr at 150 °C for 16 h, and then cooled down to 0 °C to give a yellow precipitate. The diazotization was achieved with adding $HBF_4$ and $NaNO_2$ (1:1 mol). The brown diazonium tetrafluoroborate was filtered, washed with 5 % $NaBF_4$ and $CH_3OH$, and dried under vacuum. Second, electrografting of aryl layers from diazonium salt. CFs was washed with acetone, 1 M·$HNO_3$, and deionized water, and then dried under vacuum. After 0.5 g CFs (eight trusses) and 0.015 g D1 were added into 30 mL 0.1 M $NBu_4BF_4$/ACN, electrochemical grafting of D1 was achieved on CFs at −0.30 V for 5 min; the aryl initiator modified CFs was served as eATRP macro-initiators (signed CFs–Br). Third, surface-confined eATRP. The reaction was performed at the surface of CFs–Br in 35 mL pH 7.4 PBS/$CH_3OH$ (v/v 6:1) solution containing 0.0078 g $CuBr_2$, 0.011 g 2,2′-

**Table 1** Composition (M) and pH value of the model spent bath pH 4.8

| $NiSO_4$ | $Na_2SO_4$ | $NaH_2PO_2$ | $NaH_2PO_2$ | Lactic acid | $H_2SO_4$ | $Na_2HPO_3$ |
|---|---|---|---|---|---|---|
| 0.171 | 0.38 | 0.26 | 0.26 | 0.32 | 0.19 | 0.72 |

**Table 2** Physical and textural properties of CCFs

| Sample | Surface area $m^2\ g^{-1}$ | Pore volume $cm^3\ g^{-1}$ | Pore diameter nm | Water content % |
|---|---|---|---|---|
| CCFs | 1320 | 0.41 | 47 ± 20 | 2.7 ± 0.5 |
| CFs | 1013 | 0.28 | 3 ± 1 | 1.2 ± 0.1 |

bipyridine (Bpy), and 0.5 g GMA. CuBr/Bpy complex was generated by cyclic voltammetry (CV) method with one-electron reduction of $CuBr_2$/Bpy in a 0 to −1.5 V and continuous 30 cycles, the resulting polymer modified CFs were labeled as PGMA/CFs, which were washed using acetone and deionized water, and then dried under vacuum [9]. Finally, post-functionalization of poly(glycidyl methacrylate)grafts by iminodiacetic acid attack of the epoxy groups [25]. 0.5 g PGMA/CFs (eight trusses), 0.4 g iminodiacetic acid, 3.18 g $Na_2CO_3$, and 0.2 g NaCl were added in 30 mL deionized water, and pH was adjusted to 12 using 0.1 M NaOH, which were mildly stirred for 48 h at 75 °C. The resulting material was labeled as CCFs, washed with acetone and deionized water, and then dried under vacuum.

### 2.3 Physical and textural properties

The physical and textural properties of CCFs were further investigated, and the results are summarized in Table 2 (S2). The surface area of CCFs (1320 $m^2\ g^{-1}$) is larger than that of CFs (1013 $m^2\ g^{-1}$). Moreover, water regain factor was investigated; W % represents the percentage of water held intrinsically by MFT/CFs. For water regain determination, CCFs samples were dried at 50–60 °C until they were completely dry and then weighed again. To calculate this factor, the following Eq. (2) was applied, where $W_w$ and $W_d$ are the weights (g) of the wet and dried carbon fibers, respectively. Water regain values are about 0 % for CFs, (1.1 ± 0.1) % for acid treated CFs, and (2.7 ± 0.5) % for CCFs, suggesting an improved hydrophilic character; it is advantageous for $Ni^{2+}$ adsorption, which exists in aqueous solution.

$$W\,\% = 100\,(W_w - W_d)/W_w \tag{2}$$

### 2.4 The adsorption of $Ni^{2+}$ at CCFs

The adsorption mechanism of $Ni^{2+}$ at CCFs could be suggested in Fig. 1, (2). Uptake of $Ni^{2+}$ was determined as a function of temperature, time, and pH, the value of which was adjusted using $HNO_3$ (1 M) or NaOH (0.1 M). The adsorption capacity (q, mM $g^{-1}$) of nickel was calculated using Eq. (1):

$$q = (c_0 - c_e)\,V/m \tag{1}$$

where $c_0$ and $c_e$ are the initial and equilibrium concentrations of $Ni^{2+}$ (mM $L^{-1}$), respectively; m is the mass of chelating material (g); and $V(L)$ is the volume of the solution. $c_e$ was determined by EDTA titration [26]. The initial 4.8 pH value of the spent EN plating baths were diluted and adjusted from 3.5 to 6 by the addition of $HNO_3$ and NaOH.

### 2.5 Preparation of Ni/CCFs

The formation of Ni/CCF could be seen in Fig. 1, (3). 20 mL spent EN plating baths was adjusted by 0.1 M NaOH at pH 5.2, and 0.1 mL 1 mM $PdCl_2$ (or 1 mL 30 % $H_2O_2$) was added to form dissociative $Ni^{2+}$. 0.5 g (eight trusses) CCFs immerged in the solution to adsorb $Ni^{2+}$ at 50 °C for 40 min. After washing with deionized water, the CCFs adsorbed $Ni^{2+}$ were used as working electrode at a potential of −0.7 V for 30 s in 0.5 M $H_2SO_4$ to obtain nano-nickel coated CFs (labeled as Ni/CCFs).

## 3 Result and discussion

### 3.1 Characterization of CCFs

As shown in Fig. 2a, the reduction potential of diazonium salt could be found at −0.37 V (b) in inset, implying a proper conditions for electro-graft of aryl layers at CFs (curve a matched to bare CFs). With the electro-graft of aryl layers at CFs (−0.37 V, 300 s), the current responses are obviously decreasing because the increasing aryl initiator inhibits electron transfer at CFs, suggesting the formation of CFs–Br (eATRP initiating group). Figure 2b shows the polymerization of glycidyl methacrylete (GMA) using CV method. One pair of redox peaks match to interconversion of $CuBr_2$/Bpy to CuBr/Bpy at CFs–Br, which initiates the polymerization with a surface-confined eATRP (labeled as PGMA/CFs). The currents are gradually decreasing with successive cycle at PGMA/CFs with 1 (a), 20 (b), 30 (c), and 40 (d) cycles. It probably relates alternative reason: the more the polymer is, the more the

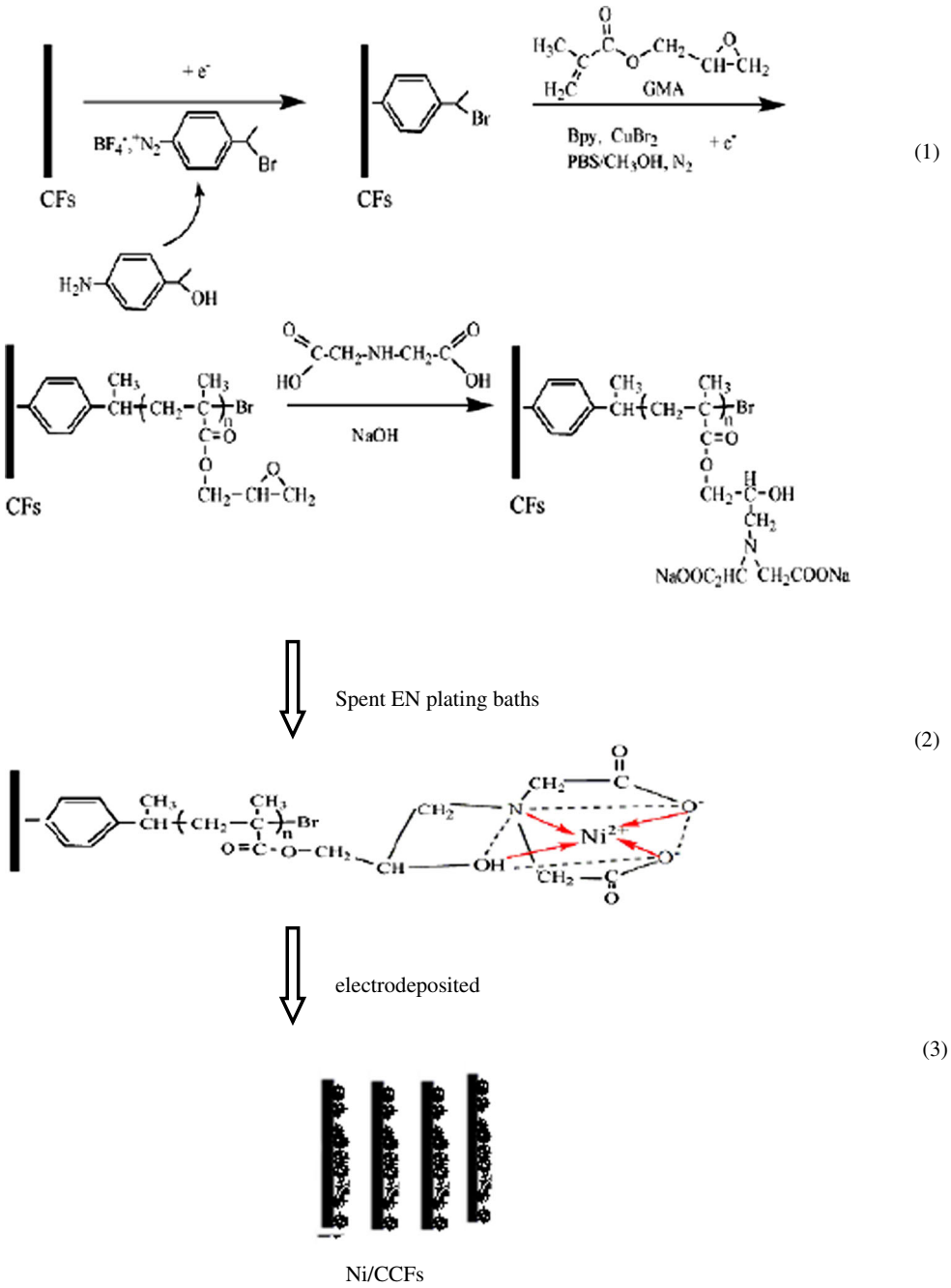


**Fig. 1** Strategy for the preparation of CCFs

mass transfer resistance is. The present polymer is nonconducting, which could inhibit the interconversion from $CuBr_2$/Bpy to CuBr/Bpy. As shown in Fig. 2c, after forming in continuous 10 (a), 20 (b), and 40 (c) cycles, PGMA/CFs were moved in 0.1 M PBS/$CH_3OH$ (v/v 6:1), and no peaks (CuBr/$CuBr_2$) could be observed; it illustrates that both $CuBr_2$/Bpy and CuBr/Bpy do not adhere at the surface of PGMA/CFs. It is notable that the background current is decreasing, which could be attributed to the increasing nonconducting polymer.

Figure 3 shows CVs (a) and electrochemical impedance spectroscopies (b) of CFs (inset a), CFs–Br (inset b), PGMA/CFs (inset c), and CCFs (d, formed at continuous 40 cycles) at 0.5 M $Fe(CN)_6^{4-/3-}$. With the progressive modification at the CFs, the redox peak currents are successively decreasing, and the impedances are gradually increasing; these imply an enhanced inhibition for the electron transfer of $Fe(CN)_6^{4-/3-}$. It is noticed that the impedance at CCFs (d 290.3 Ω) is far away bigger than that of another electrodes (a 0.5 Ω; b 3.5 Ω; and c 7.9 Ω), and the current response is the least; these

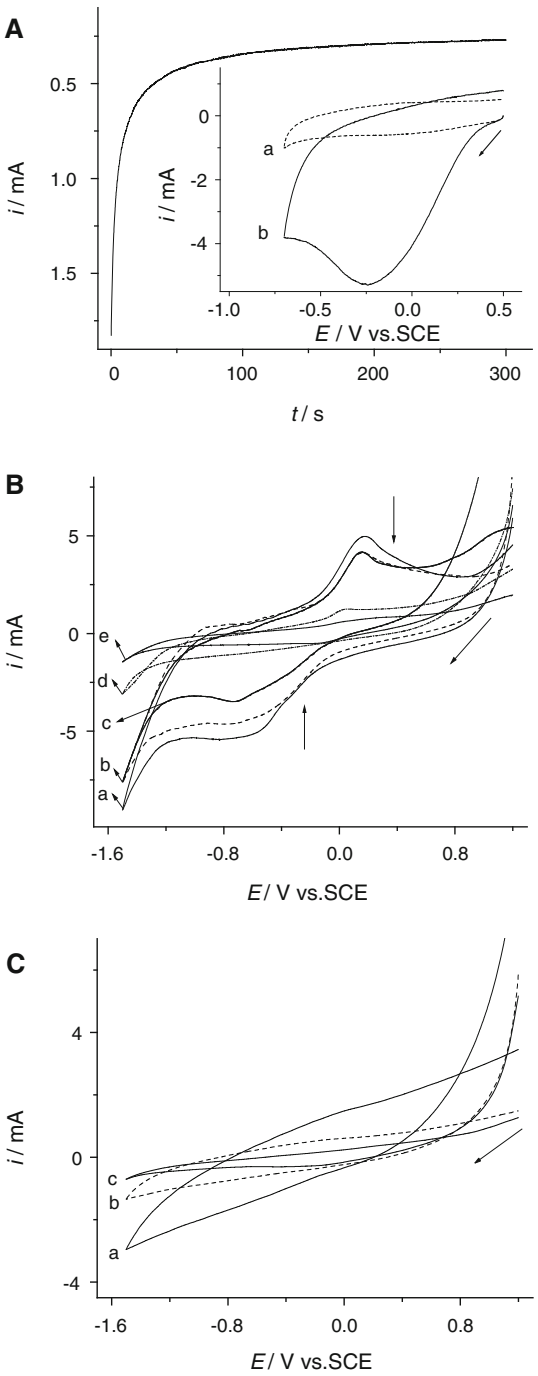


**Fig. 2** **a** CFs was treated by diazonium salt via chronoamperometry at −0.30 V for 5 min. Pulse width 0.25 s; Sample interval 0.001 s. *Inset* CVs of D1 at CFs; Scan rate: 20 $mV.s^{-1}$. Solution: ACN/0.1 M $NBu_4BF_4$. **b** CVs of $CuBr_2$/Bpy to CuBr/Bpy at CFs–Br with continuous 1st (*a*), 20th (*b*), 30th (*c*), and 40th (*d*) cycle. Solution: 0.0078 g $CuBr_2$, 0.011 g 2,2′-bipyridine (Bpy) and 0.5 g GMA/35 mL pH 7.4, 0.1 M PBS/$CH_3OH$ (v/v 6:1). Scan rate: 50 mV $s^{-1}$. **c** CVs of PGMA/CFs after formed in continuous 10 (*a*), 20 (*b*), and 40 (*c*) cycles in blank pH 7.4 0.1 M PBS/$CH_3OH$ (v/v 6:1)

illustrate that the iminodiacetic acid with negative charge could powerfully restrain the redox of $Fe(CN)_6^{4-/3-}$ at CCFs, and suggesting the formation of CCFs.

Figure 4 shows the IR spectra of relative materials such as diazonium salt (a), CFs–Br (b), PGMA/CFs (c), iminodiacetic acid (d), and CCFs (e). The vibration band at 2262 $cm^{-1}$ is the characteristic band of $N_2^+$group at diazonium salt in curve a, the peaks centered at 1579 and 1508 $cm^{-1}$ are ring vibrations of the aromatic ring, 1083 $cm^{-1}$ is in-plane CH vibrations, and 834, 793 and 700 $cm^{-1}$ are the out-of-plane-CH vibrations [25]. These bands still could be observed except characteristic band of $N_2^+$ group at CFs–Br (b) due to the immobilization of aryl initiator (–$C_6H_4$–$CH(CH_3)$–Br). The absorption bands at 1731 and 906 $cm^{-1}$ were caused by stretching vibrations of the ester carbonyl and epoxy bond at PGMA/CFs (c) [27]. After grafting iminodiacetate acid anions at PGMA/CFs, the bands at about 1715 $cm^{-1}$ of the stretching vibration of C=O in iminodiacetic acid (d) shifted to lower frequency 1630 and 1400 $cm^{-1}$ (e), and it confirms that the–COOH groups were converted into–$COO^-$ [28–30].

### 3.2 Characterization of Ni/CCFs

Figure 5a shows FE–SEM of bare CFs (inset a), and CCFs formed by PGMA/CFs at continuous 40 (b) and 60 cycles (inset b). The surface of original CFs is smooth, the polymer brushes grow monotonously at the surface of CCFs in continuous 40 cycles; the resulting thickness for polymer bushes overlap after continuous 60 cycles, and the diameter was increased from 7 to 8 μm.

After CCFs were immersed in the spent EN planting bath to adsorb $Ni^{2+}$ under pH 5.2, 35 °C and 60 min, $Ni^{2+}$ was reduced to Ni at CCFs in situ (−0.7 V for 30 s, 0.1 M $H_2SO_4$), plentiful nano-islands could be readily seen at Ni/CCFs with a size of 80 ± 10 nm in Fig. 5b and inset, signifying the formation of nano-nickel at CCFs. XRD of Ni/CFs confirms the presence of nickel nano-particles in Fig. 6. The peak at 43.9° could be assigned to $Ni^{2+}$, and the most common nano-particles are face-centered cubic. The average crystallite size is 4.9 ± 0.4 nm using Scherrer's equation from the width at half peak maximum, suggesting an aggregative state of nano-nickel at CCFs.

Optimum preparation conditions of Ni/CCFs were investigated using the spent EN planting baths at initial concentration of 17.1 mM. Figure 7 shows that the adsorption capacity of $Ni^{2+}$ at CCFs is increased with increasing pH, and it reaches a maximum value of 0.848 m $Mg^{-1}$ at pH 5.2, 35 °C, and 60 min. It is probably relative to the synergy between electrostatic interaction and ligand chelation. $Ni^{2+}$ will be hydrolyzed with the decrease of adsorption capacity at pH > 6 [20]. The adsorption capacity is gradually increased with increasing temperature until reaching a maximum value of 0.908 mM $g^{-1}$ at 50 °C, pH 5.2, and 60 min (inset a), and the increase is slow after 40 min (0.894 mM $g^{-1}$) at pH 5.2 and 50 °C (inset b). Thus, the optimum pH, temperature, and time are

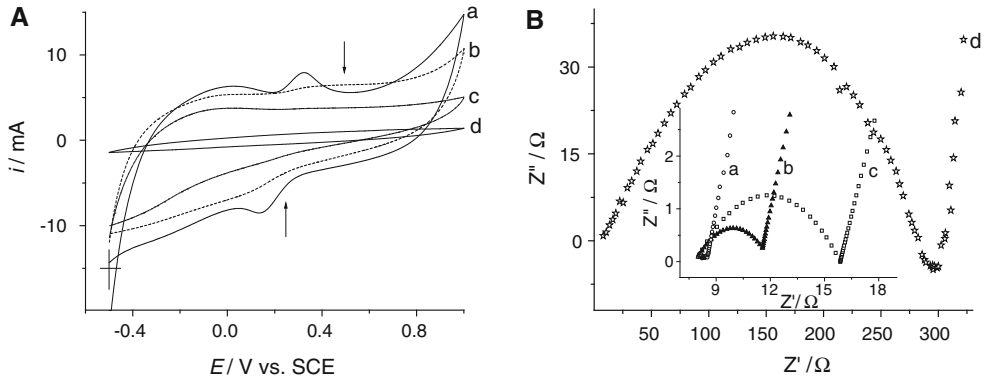


**Fig. 3** **a** CVs of CFs (*a*), CFs–Br (*b*), PGMA/CFs (*c*), and CCFs (*d*, 40th cycle). **b** Electrochemical impedance spectroscopy of CFs (*inset a*), CFs–Br (*inset b*), PGMA/CFs (*inset c*), and CCFs (*d*, 40th cycle). Solution: 0.5 M $Fe(CN)_6^{4-/3-}$/0.1 M KCl. Scan rate: 50 mV $s^{-1}$

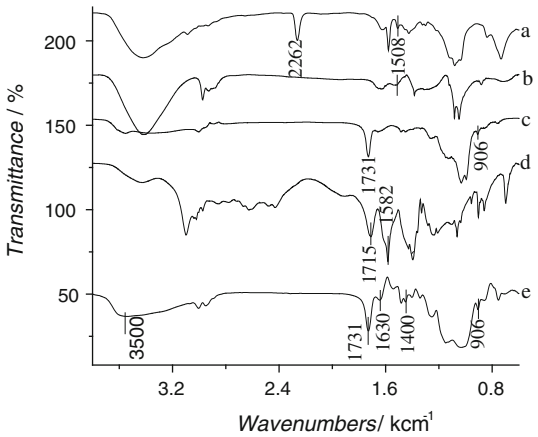


**Fig. 4** IR spectra of relative materials including diazonium salt (*a*), CFs–Br (*b*), PGMA/CFs (*c*), iminodiacetic acid (*d*), and CCFs (*e*)

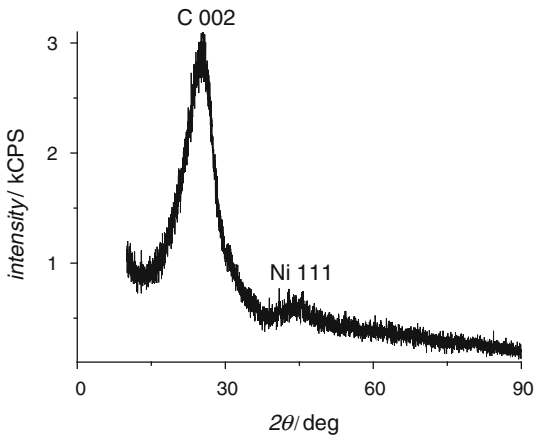


**Fig. 6** XRD of Ni/CCFs

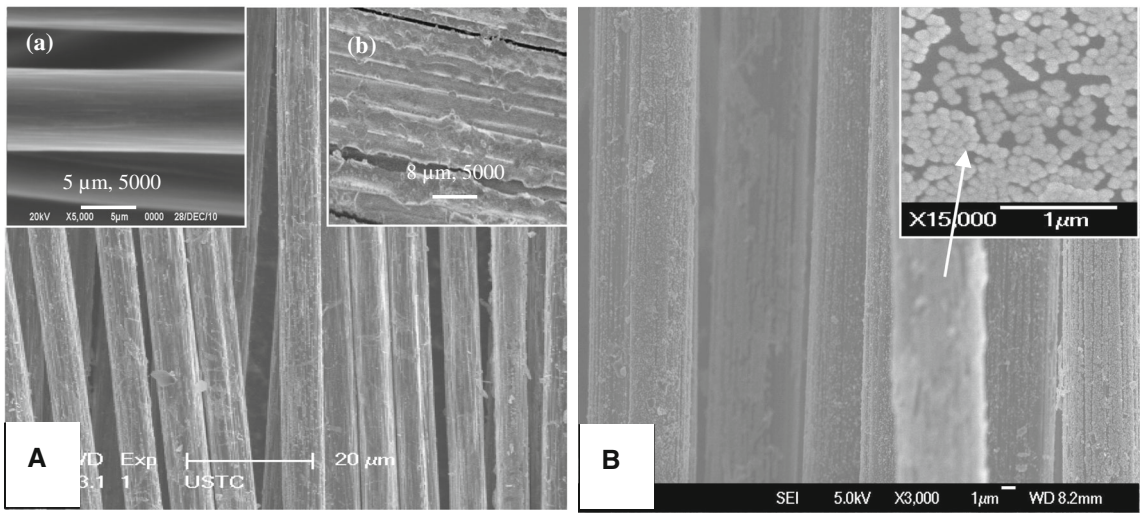


**Fig. 5** **a** SEM of bare CFs (*inset a*), CCFs formed by PGMA/CFs at 40 (*b*) and 80 cycles (*inset b*). **b** SEM of Ni/CCFs, CCFs formed by PGMA/CFs at 40 cycles

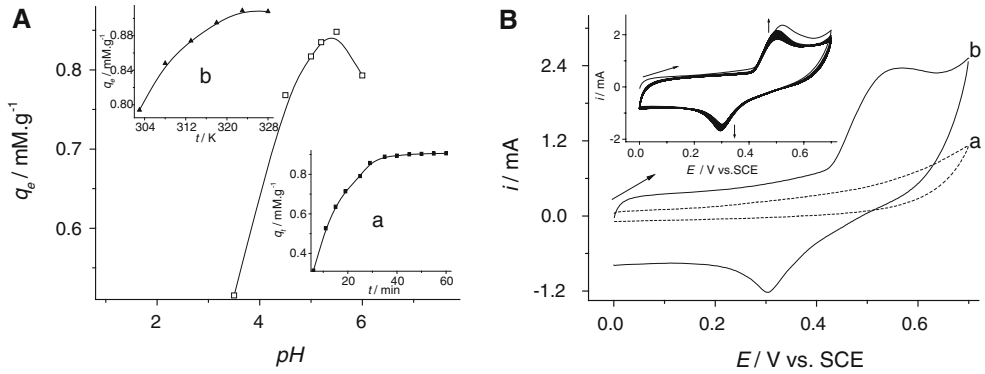


**Fig. 7** **a** Adsorption capacity of $Ni^{2+}$ at CCFs depends on pH, adsorption time (*a*) and adsorption temperature (*b*). Initial $[Ni^{2+}] = 17.1$ mM in spent EN plating bath. **b** CVs of Ni/CCFs (*inset*), 40th CVs of Ni/CCFs (*b*) and CCFs (*a*). Solution: 0.1 M NaOH

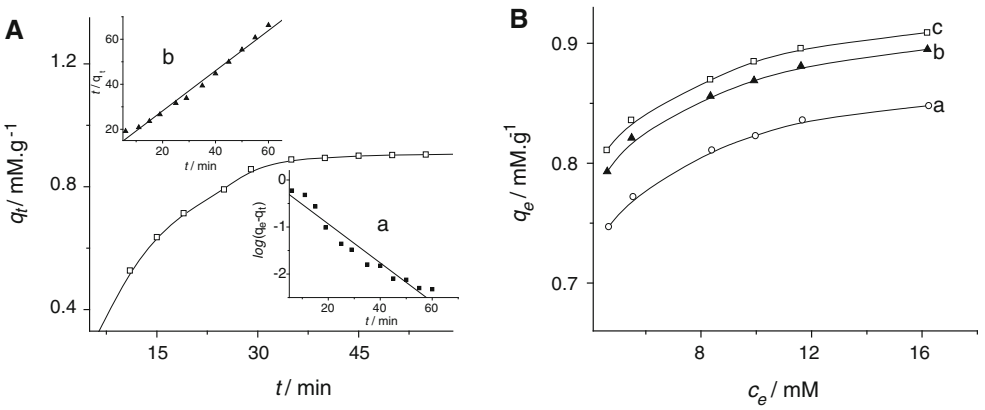


**Fig. 8** **a** The uptake of $Ni^{2+}$ depend on time at CCFs at pH 5.2 and 50 °C. *Inset* (*a*) Pseudo-first order kinetics of the uptake of $Ni^{2+}$ at CCFs. (*b*) Pseudo-second order kinetics of the uptake of $Ni^{2+}$ at CCFs. **b** Adsorption isotherms for the adsorption of $Ni^{2+}$ at CCFs at 35 (*a*), 45 (*b*), and 50 °C (*c*) at pH 5.2 and 40 min. Initial $[Ni^{2+}] = 17.1$ mM in the spent electroless plating bath

5.2, 50 °C, and 40 min, respectively. After the CCFs immersed in the spent EN planting bath under above optimum conditions, the $Ni^{2+}$ adsorbed by CCFs was electrodeposited in situ to obtain Ni/CCFs. As can be seen in Fig. 7b, inset, there are a pair of redox peaks (0.55/0.31 V) at Ni/CCFs matching to the transformation of $NiOOH/Ni(OH)_2$ in 0.1 M NaOH [2]; the responses are gradually increasing until 40 cycles, and curve b shows the 40th CV of Ni/CCFs in 0.1 M NaOH. As a comparison, after the acid treated CFs were performed by same processes, there are no responses in curve a, and it illustrates that CCFs displays an excellent uptake to $Ni^{2+}$ from the spent EN planting bath.

### 3.3 Adsorb behaviors of $Ni^{2+}$ at CCFs in spent EN planting bath

#### *3.3.1 Kinetics*

The kinetics of $Ni^{2+}$ removal at CCFs was investigated at initial concentrations of $[Ni^{2+}] = 17.1$ mM, pH 5.2, and 50 °C. Figure 8a shows that the uptake equilibrium of $Ni^{2+}$ reached within 40 min, and about 98 % of the maximum uptake capacity could be achieved. The adsorption time data were treated according to pseudo-first order in Eq. (3) and pseudo-second order in Eq. (4) [31, 32].

$$\log(q_e - q_t) = \log q_e - (k_1/2.303)t \quad (3)$$

where $k_1$ is the pseudo-first order rate constant ($min^{-1}$) of adsorption, and $q_e$ and $q_t$ (mM $g^{-1}$) are the amounts of metal ion adsorbed at equilibrium and time $t$ (min), respectively.

$$t/q_t = 1/k_2 q_e^2 + (1/q_e)t \quad (4)$$

where $k_2$ is the pseudo-second order rate constant of adsorption (g $mM^{-1}$ $min^{-1}$). The kinetic parameters for the pseudo-first and pseudo-second models were determined from the linear plots of log ($q_e$–$q_t$) vs $t$ (inset a) or ($t/q_t$) vs $t$ (inset b), respectively. The validity of each model could be checked by the fitness of the straight lines ($R^2$ values). Accordingly, as shown in Table 3 (S3), the adsorption of $Ni^{2+}$ on CCFs perfectly fits the pseudo-

**Table 3** Parameters of the pseudo-first order and the pseudo-second order for the adsorption of $Ni^{2+}$ on CCFs. Initial $[Ni^{2+}] = 17.1$ mM

| Metal ion | $Q_{e,exp}$ (mM $g^{-1}$) | Pseudo-first order | | | Pseudo-second order | | |
|---|---|---|---|---|---|---|---|
| | | $k_1$ ($min^{-1}$) | $q_e$ (mM $g^{-1}$) | $R^2$ | $k_2$ (g $mM^{-1}$ $min^{-1}$) | $q_e$ (mM $g^{-1}$) | $R^2$ |
| $Ni^{2+}$ | 0.908 | 0.105 | 1.20 | 0.971 | 0.077 | 1.12 | 0.993 |

**Table 4** Langmuir constants for adsorption of $Ni^{2+}$ on CCFs. Initial $[Ni^{2+}] = 17.1$ mM

| T/ °C | $Q_{max}$ (mM $g^{-1}$) | $K_L$(L $mM^{-1}$) | $R^2$ |
|---|---|---|---|
| 35 | 0.909 | 1.15 | 0.999 |
| 45 | 0.943 | 1.22 | 0.999 |
| 50 | 0.952 | 1.27 | 0.999 |

second order model ($R^2 = 0.993$) rather than the pseudo-first order one ($R^2 = 0.971$). When the pseudo-second-order model is the best fit for the experimental data, the sorption mechanism involved chemisorption, which could be suggested in Fig. 1, (2) [2, 26].

### 3.3.2 Adsorption isotherms

The adsorption isotherm of $Ni^{2+}$ at CCFs was investigated at 35, 45, and 50 °C in Fig. 8b. The adsorption curves show the highest uptake values for $Ni^{2+}$ at 0.908 mM $g^{-1}$ and at 50 °C. The adsorption data were plotted according to Langmuir equation (5).

$$c_e/q_e = c_e/Q_{max} + 1/K_l Q_{max} \quad (5)$$

where $c_e$ is the concentration of metal ions in solution (mM), $q_e$ is the metal ions concentration in the resin phase at CCFs (mM $g^{-1}$), $Q_{max}$ is the maximum adsorption capacity (mM $g^{-1}$), and $K_L$ is the Langmuir binding constant which is related to the energy of adsorption (L $mM^{-1}$). All concentrations refer to equilibrium conditions. The value of $Q_{max}$ (obtained from Langmuir plots) at 50 °C is mainly consistent with that experimentally obtained, indicating that the adsorption process is mainly monolayer. The obvious increase in both values of $Q_{max}$ and $K_L$ at elevated temperature indicates the endothermic nature of the adsorption process in Table 4 (S4).

## 4 Conclusions

Iminodiacetic acid modified poly(glycidyl methacrylete) grafted carbon fibers were first obtained by electrochemically mediated atom transfer radical polymerization using aryl diazonium salt initiators. Kinetic and thermodynamics studies showed that the functional carbon fibers could intensively adsorb $Ni^{2+}$ from the spent EN plating baths, and then nano-nickel coated-carbon fibers material could be formed by electrodeposition in situ. This work provided an efficient approach for the new preparation of chelating carbon fibers and application in heavy metal wastewater treatment.

**Acknowledgments** This work was supported by the National Natural Science Foundation of China (NSFC, 21076054 and 21174001), Natural Science Important Foundation of Educational Commission of Anhui Province (2010AJZR-85, 2011AJZR-87), Study Foundation of New Product and Technology of Anhui Economic and Information Technology Commission (2012AHST0797), and National College Student Innovation Fund (201210359034, 2013CXSY327 and 2013 CXSY366).

## References

1. Kadirvelu C, Faur-Brasquet C, Cloirec PL (2000) Langmuir 16:8404
2. Jin GP, Wang XL, Fu Y, Dou Y (2012) Chem Eng J 203:440
3. Kaiser J (2002) Science 296:452
4. Dwivedi P, Gaur V, Sharma A, Verma N (2004) Sep Purif Technol 39:23
5. Kraemer SM, Xu JD, Raymond KN, Sposito G (2002) Environ Sci Technol 36:1287
6. Ribeiro MHL, Ribeiro IAC (2005) Sep Purif Technol 45:232
7. Saeed A, Akhter MW, Iqbal M (2005) Sep Purif Technol 45:25
8. Sinha-Ray S, Khansari S, Yarin AL, Pourdeyhimi B (2012) Ind Eng Chem Res 51:109
9. Chergui SM, Abbas N, Matrab T (2010) Carbon 48:2106
10. Li G, Zhang L, Li Z, Zhang W (2010) J Hazard Mater 177:983
11. Ma N, Yang Y, Chen S, Zhang Q (2009) J Hazard Mater 171:288
12. Magenau AJD, Strandwitz NC, Gennaro A, Matyjaszewski K (2011) Science 332:81
13. Kato M, Kamigaito M (1995) Macromolecules 28:1721
14. Wang JS, Matyjaszewski K (1995) Macromolecules 28:7901
15. Li B, Yu B, Huck WTS, Zhou F, Liu W (2012) Angew Chem Int Ed 51:5092
16. Dong H, Tang W, Matyjaszewski K (2007) Macromolecules 40:2974
17. Peng L, Su Z (2005) Polym Int 54:1508
18. Ghislandi M, Prado LASDA, Oyerviedes ADLV, Wittich H, Schulte K (2008) J Polym Sci Pol Chem 46:3326
19. Li L, Lukehart CM (2006) Chem Mater 18:94
20. Chiang CL, Huang PC, Chen CY (2006) Sep Purif Technol 50:15
21. Wang CC, Chen CY, Chang CY (2002) J Appl Polym Sci 84:1353
22. Chen CY, Chang CY (2002) J Appl Polym Sci 86:1986
23. Chen CY, Chiang CL (2008) Mater Lett 62:3607
24. Zhang M, Zhang W (2008) J Phys Chem C 112:6245
25. Matrab T, Chehimi MM (2005) Langmuir 21:4686
26. El-Ghaffar MAA, Abdel-Wahab ZH (2009) Hydrometallurgy 96:27

27. Lei QJ, Gao BJ (2011) Acta Phys Chim Sin 27:2697
28. Hou WH, Chen CY (2003) Electrochim Acta 48:679
29. Chu YC, Wang CC, Huang YH, Chen CY (2005) Nanotechnology 16:376
30. Wang L, Xu X, Evans DG, Duan X, Li D (2010) J Solid State Electrochem 183:1114
31. Lagergren S (1898) Handlingar 24:1
32. Ho YS, McKay G (1999) Process Biochem 34:451